04

# Tokamak EAST edge plasma modeling with SOLPS-ITER3.2.0 on the wide grid with account of drifts

© N.V. Shtyrkhunov[1], I.Yu. Senichenkov[1], E.G. Kaveeva[1], V.A. Rozhansky[1], R. Ding[2], H. Si[2], G. Xu[2], J. Guo[2]

[1] Peter the Great Saint-Petersburg Polytechnic University, St. Petersburg, Russia
[2] Institute of Plasma Physics, Chinese Academy of Sciences, Hefei, PRC
E-mail: E.Kaveeva@spbstu.ru

*Received October 15, 2024*
*Revised November 20, 2024*
*Accepted November 20, 2024*

The modeling results for tokamak EAST are presented obtained with the new version of SOLPS-ITER 3.2.0 code specially designed for the edge plasma transport description up to the camber wall with the account of its shape. For the first time the modeling with account of ExB drift and diamagnetic drift in the inhomogeneous magnetic field is performed on the unstructured grid including triangle cells in the chamber wall vicinity. The electrostatic potential distribution is obtained. The modeling results are compared with experiment, with the calculation on the narrower structured grid, and with the calculation without drifts.

**Keywords:** SOLPS-ITER, EAST, wide grid, drifts.

DOI: 10.61011/TPL.2025.04.60988.20150

The characterization of interaction of ions and neutral atoms with the first wall is a topical problem in the physics of controlled thermonuclear fusion [1]. Sputtering of the chamber wall affects its service lifetime and leads to contamination of plasma with impurities. Fluxes of atoms to the chamber walls may be used for diagnostic purposes.

Hydrodynamic codes are used widely to characterize the divertor and scrape-off layer (SOL) plasmas. The most popular and best-proven by comparison with the experimental data is the SOLPS-ITER [2] code. The standard SOLPS-ITER simulation domain includes a plasma layer few centimeters in width in the scrape-off layer and is bounded by a constant poloidal flux surface that does not coincide with the chamber wall. The same computational domain is used for the hydrodynamic characterization of both neutral particles and plasma. If the EIRENE code for Monte Carlo calculations of the distribution of neutral particles is connected, the calculation area for neutral particles may be extended to the chamber wall. SOLPS-ITER 3.2.0 [3] has been released recently. This version allows one to construct a grid and extend to the first wall the computational domain within which the plasma equations are solved. This extension necessitated a change in the data structure of the code, the introduction of triangular cells into the computational grid, and the emergence of short magnetic tubes with a low plasma density near the walls. All this introduced additional numerical difficulties. The first examples of modeling with the new version of the code for the EAST tokamak were presented in [4]. The authors of this paper have managed to obtain solutions with account for drifts on a standard grid, which did not extend to the chamber walls, and a solution without drifts on a grid extending to the walls. In the present study, we report the results of the first simulation that uses a grid reaching the chamber wall and takes all drift fluxes into account. The grid was transformed for this purpose, and the boundary conditions (in particular, the interpolation of drift fluxes) were improved.

The calculation corresponds to the ohmic L-mode of the EAST tokamak in a configuration with two $X$-points, an active lower $X$-point, and a distance of 1.8 cm between the separatrices. The gradient drift of ions is directed downward.

The following anomalous transport coefficients were set: $D_{AN} = 0.8\,\mathrm{m}^2/\mathrm{s}$, $\chi_{AN,i} = \chi_{AN,e} = 1.0\,\mathrm{m}^2/\mathrm{s}$, and $V_{AN} = 2\,\mathrm{m/s}$. Density $n_e = 1.15 \cdot 10^{19}\,\mathrm{m}^{-3}$ and temperatures $T_e = T_i = 250\,\mathrm{eV}$, which are consistent with the experimental data, were set at the boundary of the computational domain inside the separatrix. The rate of gas supply from the chamber wall was $10^{21}$ atoms/s. Atoms were characterized in the improved hydrodynamic approximation [5] that is featured in SOLPS-ITER 3.2.0 but is unavailable in the standard SOLPS-ITER. The model of energy exchange between atoms and the wall was improved significantly in this approximation. The results of three calculations with the SOLPS-ITER 3.2.0 code are presented below. Drifts were neglected in the first one. The other two included drift terms on the old structured (narrow) and new unstructured (wide) grids. The calculation on the old grid differs from the one denoted as „DDN wide att" in [4] in that the improved hydrodynamic model for atoms was used. The preservation of plate parameters corresponding to the experimental ones necessitated a slight alteration of the vacuum pumping parameters and a reduction of the anomalous diffusion coefficient (in [4], $D_{AN} = 1.0\,\mathrm{m}^2/\mathrm{s}$). Feedback was included in the simulation to adjust the vacuum pumping so that the pressure of atoms in the divertor would provide a recycling

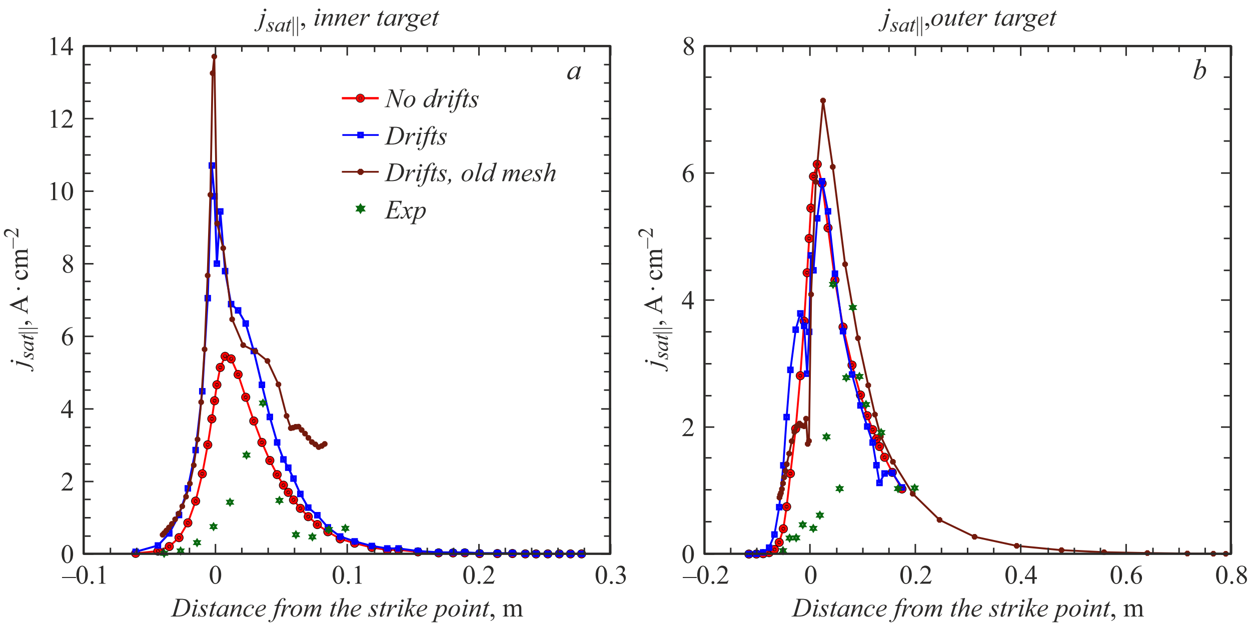


**Figure 1.** Ion saturation current at divertor plates determined in calculations without and with drifts on the unstructured grid, in calculations with drifts on the structured grid, and in probe measurements as a function of distance to the point of intersection with the plate separatrix. Positive values on the abscissa axis correspond to the region outside the separatrix.

level suitable for maintaining an electron temperature at the outer plate corresponding to the experimental one (32 eV at the maximum). This is the reason why the temperatures at the outer plate are the same in all three calculations. The saturation current at the inner and outer divertor plates is shown in Figs. 1, *a* and *b*. While all three calculations yield similar results for the outer plate, significant differences are found at the inner one. This is seen also in Fig. 2, which presents the electron density distributions for four calculations (the fourth one was denoted as „DDN wide att 3.0.8"in [4]). Just as in [4], the density at the inner divertor increases when drifts are enabled on the wide grid. The formation of a region of high density in the inner divertor, which was observed both in modeling and in experiments [6] (high-field side high density), is initiated. However, this region on the narrow grid with drifts is much more pronounced than on the wide one. These results are illustrated by the table that lists the number of ions within the inner and outer divertors below the $X$-point (including the corresponding part of the region between the separatrices below the $X$-point). It can be seen that the number of particles in the inner divertor increases by 60% when drifts are enabled on the wide grid. The enhancement on the narrow grid is even more pronounced. At the same time, the number of particles in the outer divertor changes insignificantly between calculations, provided that the temperatures at the outer plate remain the same.

Artificial narrowing of the computational domain in the simulation is equivalent to installing reflectors, which would make the divertor more closed, in the experiment. Experiments with such reflectors at the TCV tokamak have revealed that they facilitate the transition to the detachment regime [7]. Atoms produced during recycling remain in the divertor for longer, contribute to its cooling, and are more likely to be ionized again in the divertor if reflectors are installed. Recycling also proceeds at the reflectors themselves. Cold plasma regions turn out to be denser due to the preservation of pressure along the magnetic tubes. Cooling of the inner divertor also leads to an increase in its electrical resistance and an enhancement of the electric field associated with the thermoelectric current. Drift fluxes are intensified in this case, raising the density in the inner divertor. It is instructive to compare the simulation results with the calculation performed with the SOLPS-ITER 3.0.8 code [4] and presented in Fig. 2, *d*. The boundary of the computational domain for plasma in this calculation matched the narrow grid (Fig. 2, *c*), while the domain for EIRENE atomic simulation was wide. The region with increased density in Fig. 2, *d* is narrower than in panel *c*, but wider than in panel *b*.

We note in conclusion that the first results of modeling with the SOLPS-ITER 3.2.0 numerical code on an extended unstructured grid with drifts taken into account were obtained and found to agree with the data from an experiment at the EAST tokamak in the L-mode. It was demonstrated that the introduction of drifts has a significant effect on the parameters in the divertor region and the difference in plasma densities near the plates, while the profiles in the equatorial plane remain virtually unchanged. In future studies, this simulation is planned to be carried out with a kinetic description of neutral particles instead of a hydrodynamic one.

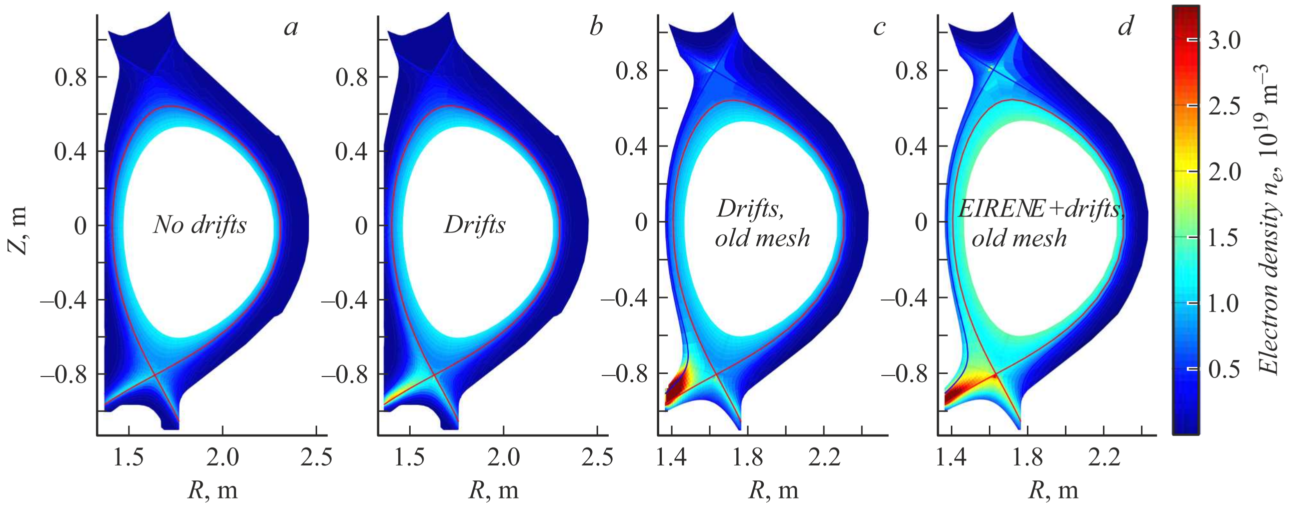


**Figure 2.** Electron density distribution for calculations on the wide grid without ($a$) and with ($b$) drifts, on the old grid with drifts ($c$), and on the old grid with drifts and the EIRENE code for atomic simulations ($d$).

Distribution of the number of ions between divertors

| Divertor | Calculation | | | |
|---|---|---|---|---|
| | Wide grid without drifts | Wide grid with drifts | Narrow grid with drifts | SOLPS-ITER3.0.8 with drifts and EIRENE |
| Inner | $2.57 \cdot 10^{18}$ | $4.16 \cdot 10^{18}$ | $7.92 \cdot 10^{18}$ | $7.95 \cdot 10^{18}$ |
| Outer | $2.41 \cdot 10^{18}$ | $2.87 \cdot 10^{18}$ | $3.21 \cdot 10^{18}$ | $4.61 \cdot 10^{18}$ |
| Total | $4.97 \cdot 10^{18}$ | $7.03 \cdot 10^{18}$ | $11.13 \cdot 10^{18}$ | $12.56 \cdot 10^{18}$ |


## Acknowledgments

Calculations were performed at the supercomputer center of Peter the Great St. Petersburg Polytechnic University.

## Funding

This study was supported by the Russian Science Foundation (23-42-00020) and the National Natural Science Foundation of China (grant 12261131496).


## Conflict of interest

The authors declare that they have no conflict of interest.

## References


[1] R.A. Pitts, X. Bonnin, F. Escourbiac, H. Frerichs, J.P. Gunn, T. Hirai, A.S. Kukushkin, E. Kaveeva, M.A. Miller, D. Moulton, V. Rozhansky, Nucl. Mater. Energy, **20**, 100696 (2019). DOI: 10.1016/j.nme.2019.100696

[2] S. Wiesen, D. Reiter, V. Kotov, M. Baelmans, W. Dekeyser, A.S. Kukushkin, S.W. Lisgo, R.A. Pitts, V. Rozhansky, G. Saibene, I. Veselova, J. Nucl. Mater., **463**, 480 (2015). DOI: 10.1016/j.jnucmat.2014.10.012

[3] W. Dekeyser, P. Boerner, S. Voskoboynikov, V.A. Rozhanksy, I. Senichenkov, L. Kaveeva, I. Veselova, E. Vekshina, X. Bonnin, R.A. Pitts, M. Baelmans, Nucl. Mater. Energy, **27**, 100999 (2021). DOI: 10.1016/j.nme.2021.100999

[4] I. Senichenkov, E. Kaveeva, V. Rozhansky, N. Shtyrkhunov, K. Dolgova, R. Ding, H. Si, G. Xu, Contribut. Plasma Phys., **64**, e202300136 (2024). DOI: 10.1002/ctpp.202300136

[5] W.V. Uytven, W. Dekeyser, M. Blommaert, S. Carli, M. Baelmans, Nucl. Fusion, **62**, 086023 (2022). DOI: 10.1088/1741-4326/ac72b4

[6] S. Potzel, M. Wischmeier, M. Bernert, R. Dux, F. Reimold, A. Scarabosio, S. Brezinsek, M. Clever, A. Huber, A. Meigs, J. Nucl. Mater., **463**, 541 (2015). DOI: 10.1016/j.jnucmat.2014.12.008

[7] O. Février, H. Reimerdes, C. Theiler, D. Brida, C. Colandrea, H. De Oliveira, B.P. Duval, D. Galassi, S. Gorno, S. Henderson, Nucl. Mater. Energy, **27**, 100977 (2021). DOI: 10.1016/j.nme.2021.100977


*Translated by D.Safin*